BIOCHEMISTRY
including biophysical chemistry & molecular biology

Article

pubs.acs.org/biochemistry

Alternative Pathways of Human Islet Amyloid Polypeptide Aggregation Distinguished by ^{19}F Nuclear Magnetic Resonance-Detected Kinetics of Monomer Consumption

Yuta Suzuki,[†] Jeffrey R. Brender,[§] Kevin Hartman,[§] Ayyalusamy Ramamoorthy,*[,†,§] and E. Neil G. Marsh*[,†,‡]

[†]Department of Chemistry, [‡]Department of Biological Chemistry, and [§]Department of Biophysics, University of Michigan, Ann Arbor, Michigan 48109, United States

Supporting Information

ABSTRACT: Amyloid formation, a complex process involving many intermediate states, is proposed to be the driving force for amyloid-related toxicity in common degenerative diseases. Unfortunately, the details of this process have been obscured by the limitations in the methods that can follow this reaction in real time. We show that alternative pathways of aggregation can be distinguished by using ^{19}F nuclear magnetic resonance (NMR) to monitor monomer consumption along with complementary measurements of fibrillogenesis. The utility of this technique is demonstrated by tracking amyloid formation in the diabetes-related islet amyloid polypeptide (IAPP). Using this technique, we show IAPP fibrillizes without an appreciable buildup of nonfibrillar intermediates, in contrast to the well-studied Aβ and α-synuclein proteins. To further develop the usage of ^{19}F NMR, we have tracked the influence of the polyphenolic amyloid inhibitor epigallocatechin gallate (EGCG) on the aggregation pathway. Polyphenols have been shown to strongly inhibit amyloid formation in many systems. However, spectroscopic measurements of amyloid inhibition by these compounds can be severely compromised by background signals and competitive binding with extrinsic probes. Using ^{19}F NMR, we show that thioflavin T strongly competes with EGCG for binding sites on IAPP fibers. By comparing the rates of monomer consumption and fiber formation, we are able to show that EGCG stabilizes nonfibrillar large aggregates during fibrillogenesis.

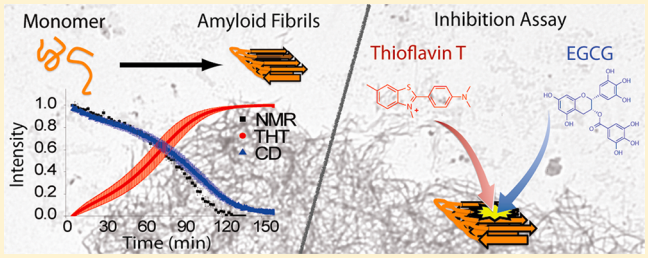

The formation of amyloid fibers is associated with a wide range of pathologies, including Alzheimer's disease, Parkinson's disease, and type II diabetes.[1] Under pathological conditions, amyloidogenic proteins self-assemble into long fibrillar structures with a characteristic β-sheet core.[2−4] Although a detailed mechanism is lacking for most amyloidogenic proteins, amyloidogenesis is believed to be a complex, multistep process, typically involving the formation of energetically unfavorable intermediates before the formation of the final amyloid product.[5−8]

Because amyloid formation is such a complex process, a full understanding of the pathology caused by amyloid formation requires establishing both the identity of intermediates along the amyloid pathway and the kinetics of their formation. The actual identity of the species responsible for toxicity is elusive and has been the subject of much debate since the discovery of amyloid plaques more than a century ago.[7−9] A current hypothesis holds that small to intermediate size (∼5−6 nm in diameter) oligomers may be responsible for much of the toxicity of amyloid proteins.[6,8] For the Aβ protein, probably the best studied amyloidogenic protein, oligomers of this type have been isolated both in vitro and in situ from tissue samples of Alzheimer's patients. While a large body of literature linking small oligomers of this type to the pathological action of other amyloidogenic proteins besides Aβ exists, their actual existence in many other amyloidogenic proteins has largely been inferred rather than directly tested.[7] For islet amyloid polypeptide (IAPP) in particular, the existence of small oligomeric species of this type is controversial.[7,8] Most attempts to detect them have used the conformation-specific antibody A11, whose specificity toward non-Aβ oligomers has been called into question,[7] as it appears to give both false positive and false negative results under some conditions.[7,10−13] Attempts to detect these oligomers directly have largely been negative, although these experiments have used an equilibrium approach that may not detect transient oligomers.[14,15] In the absence of well-defined targets, research attempting to attenuate amyloid-linked toxicity has been substantially impeded.

Toward this end, various methods have recently been exploited to monitor the kinetics of amyloid fibril formation, including fluorescence,[16−19] nuclear magnetic resonance (NMR),[20,21] two-dimensional infrared,[22,23] and mass spectroscopy.[24,25] The most common method for measuring amyloid

Received: September 13, 2012
Revised: September 20, 2012
Published: September 21, 2012

dx.doi.org/10.1021/bi3012548 | *Biochemistry* 2012, 51, 8154−8162

formation exploits the increase in fluorescence when the dye thioflavin T (ThT) binds to the fibers. Although the ThT assay is simple and relatively sensitive, it does not accurately distinguish between oligomeric species.[26] Therefore, it is not particularly useful by itself for the investigation of amyloidogenic intermediates. Similarly, reporters of secondary structures such as circular dichroism (CD), Fourier transform infrared, and multidimensional NMR spectroscopy have difficulty in detecting the underlying spectral signature of the intermediate species, which may be transient and not form a majority of the total population.

On the other hand, real-time ^{1}H NMR measurements, in theory, allow the signal from each species to be resolved and analyzed independently. Unfortunately, ^{1}H NMR is relatively insensitive to changes in structure caused by small chemical shift dispersions associated with the ^{1}H nucleus. Whereas ^{13}C and ^{15}N experiments are more sensitive to environmental changes, the low sensitivity of these nuclei makes it difficult to acquire data sufficiently rapidly to track intermediates during aggregation. In contrast, ^{19}F combines both excellent sensitivity and large chemical shift dispersion, making it an excellent reporter for changes in the chemical environment.[27,28] Thus ^{19}F NMR has been broadly applied to investigate protein conformational changes and dynamics as well as protein−ligand and protein−membrane interactions in biological systems.[29−43] Whereas the properties of ^{19}F NMR spectroscopy are attractive for amyloid research, applications to amyloid proteins have been relatively limited.[44,45] In particular, detailed time-resolved studies of protein aggregation or inhibition assays using ^{19}F NMR have not been performed.

In this report, we demonstrate the utility of ^{19}F NMR to provide a direct, sensitive, and real-time measurement of amyloid formation by the highly amyloidogenic peptide, IAPP, which is achieved by monitoring the consumption of monomeric protein rather than the formation of fibrils by dye binding. IAPP is a 37-residue peptide hormone secreted from pancreatic β-cells along with insulin to contribute glycemic control.[46] However, an insoluble fibril form of IAPP is found in the pancreas of up to 90% of patients with type II diabetes that may contribute to the pathology of the disease.[7,8,47,48] Using real-time ^{19}F NMR in combination with other techniques to measure conformational changes during the aggregation pathway, we show IAPP forms fibers from monomeric IAPP at pH 7.3 without an appreciable buildup of nonfibrillar intermediates during aggregation, in contrast to most amyloidogenic proteins.[6] However, this pathway can be altered toward the formation of nonfibrillar intermediates using inhibitors such as epigallocatechin gallate (EGCG).

MATERIALS AND METHODS

Peptide Synthesis. Peptide (IAPP-tfmF$_{23}$) was synthesized manually in the free acid form by solid-phase 9-fluorenylmethoxycarbonyl (Fmoc)-based chemistry using pseudoproline dipeptides to disrupt aggregation during synthesis, as described previously.[49] 4-Trifluoromethylphenylalanine (tfmF) was used to replace Phe at position 23. The disulfide bridge between Cys2 and Cys7 in IAPP was formed on the resin using thallium(III) trifluoroacetate as a mild oxidant and cleaved from resin using 95% trifluoroacetic acid.[49] Crude peptides were dissolved in 35% (v/v) acetic acid and purified on a reversed-phase high-performance liquid chromatography system using a Waters semipreparative C18 column equilibrated in 0.045% HCl. The peptides were eluted with a linear gradient from 0 to 80% acetonitrile at a flow rate of 10 mL/min. Peptide identity was confirmed using matrix-assisted laser desorption ionization mass spectroscopy.

Sample Preparation. To remove preformed aggregates, we dissolved the purified peptide in hexafluoro-2-propanol followed by the removal of the solvent by lyophilization. An 850 μM stock solution was made before each set of experiments by first dissolving the lyophilized peptide in 0.1 mM HCl (pH 4.0). The stock solution was then passed though a 0.22 μm filter before dilution into the final buffer solution immediately before the start of each experiment. The concentrations of peptide stock solutions were determined by the absorbance of Y37 (ε = 1215 L mol^{-1} cm^{-1} at 280 nm).[50] All experiments were performed at a constant peptide concentration of 85 μM. The final solutions contained 20 mM sodium phosphate, 50 mM NaCl (pH 7.3), 10% D_2O, and various concentrations of EGCG, ThT, and EDC/sulfo-NHS as indicated in the figure captions. For NMR measurements, ^{19}F chemical shifts were referenced to an internal standard of trifluoroethanol (100 μM TFE, at 0 ppm).

Kinetic Studies Using ^{19}F NMR Spectroscopy. All ^{19}F NMR experiments were performed using a Varian VNMRS 500 MHz NMR spectrometer equipped with a double-tuned ^{1}H−^{19}F probe. After the addition of peptide to the NMR solution, a series of ^{19}F spectra were recorded without spinning. Each ^{19}F spectrum takes 116 s using 64 transients (25 and 37 °C) or 232 s using 128 transients (10 °C) with a 1.0 s pulse delay between each transient. Line broadening of 3.0 Hz was used to process the final spectra. All of the samples were pre-equilibrated at the indicated temperatures before being mixed with the peptide stock solution. Origin 8.5 was used for plotting and fitting the data.[51]

Kinetic Studies Using Thioflavin Fluorescence. The kinetics of IAPP amyloid formation was measured using the increase in fluorescence intensity observed when the amyloid-specific dye ThT binds to the amyloid fibrils. The samples were prepared as described above for the NMR solution except that 100 μM ThT was premixed with buffer solution before the addition of peptide. Time traces were recorded with a FluoroMax-2 spectrofluorometer using a 440 nm excitation filter and a 485 nm emission filter at a constant temperature without shaking.

Circular Dichroism. CD measurements were performed with an Aviv 62DS spectropolarimeter using a 0.1 cm path length cell. The samples were prepared as described above for the NMR solution. Mean residue ellipticities, $[\theta]$, were calculated using the relationship $[\theta] = \theta_{obsd}/(10lcn)$, where θ_{obsd} is the ellipticity measured in millidegrees, c is the molar concentration, l is the cell path length in centimeters, and n is the number of residues in the peptide. Full spectra were smoothed by Savitzky−Golay smoothing (five-point window).

Electron Microscopy. Aliquots were taken directly from the NMR samples at the time points indicated. Aliquots (6 μL) were incubated onto Formvar-coated copper grids (Ernest F. Fullam, Inc., Latham, NY) for 2 min, washed five times with 6 μL of deionized water, and then negatively stained for 1 min with 2% uranyl acetate. Samples were imaged using a Philips CM10 transmission electron microscope.

RESULTS AND DISCUSSION

^{19}F NMR Sensitively Measures Monomer Consumption during Aggregation. To study fibril formation using ^{19}F NMR, we synthesized a ^{19}F-labeled IAPP (IAPP-tfmF$_{23}$) in

dx.doi.org/10.1021/bi3012548 | Biochemistry 2012, 51, 8154−8162

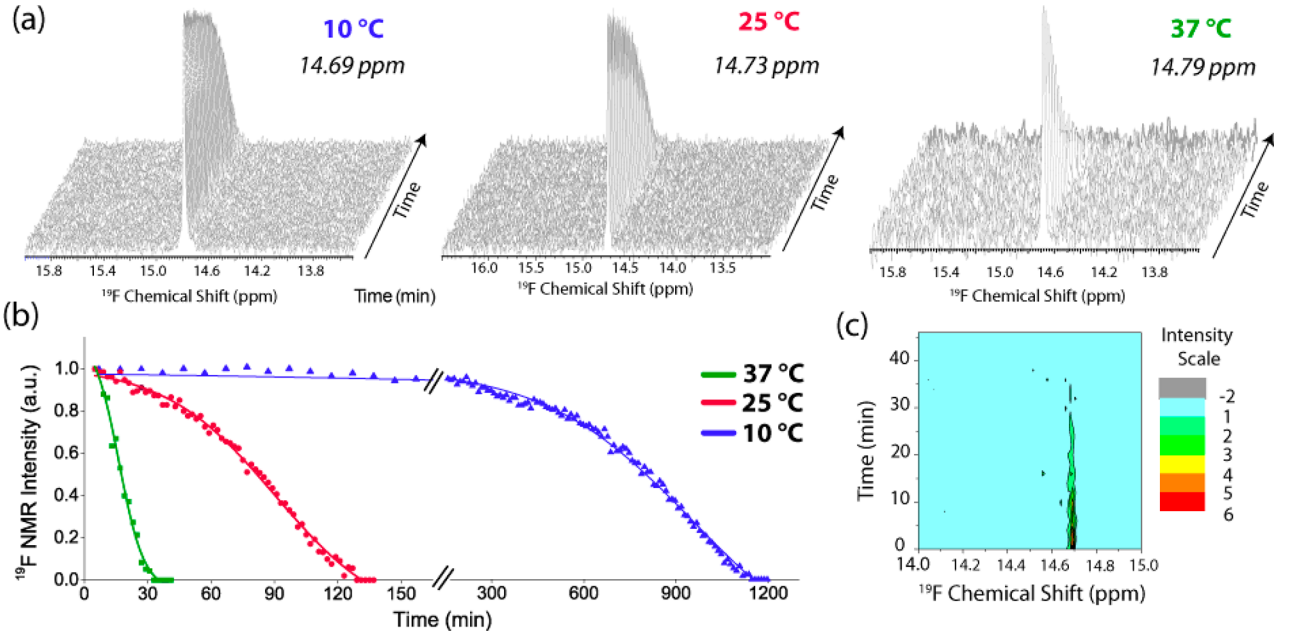

Figure 1. Kinetics of the disappearance the IAPP-tfmF$_{23}$ monomer followed by ^{19}F NMR. (a) Stacked plots of ^{19}F NMR spectra (TFE = 0.0 ppm). The experiment was conducted at 10 °C (left), 25 °C (center), and 37 °C (right) at pH 7.3. (b) Plots of peak intensity of the main resonance from panel A as a function of time. Solid lines represent sigmoidal fits to the ^{19}F data. (c) Contour plot of the ^{19}F NMR spectra at 37 °C showing the absence of new peaks.

which Phe23 is substituted with 4-trifluoromethylphenylalanine (tfmF). Phe23 is solvent-exposed in the unstructured monomeric peptide[19,52] but is believed to be become buried when the peptide forms aggregates.[2,19,53,54] The ^{19}F chemical shifts and line widths of the trifluoromethyl groups should change significantly as the peptide undergoes changes in its secondary structure and oligomerization state, as has been observed for other fluorinated peptides and proteins.[38−40] In particular, if oligomeric intermediates on the amyloid forming pathway accumulate to an appreciable extent, they should be detectable by NMR, provided they are not so large that their line widths are broadened excessively, as is the case for amyloid fibers.[20] Furthermore, the ^{19}F signal is sufficiently sensitive to monitor peptide aggregation at low concentrations that allows a direct comparison with other methods for following aggregation such as CD or fluorescence spectroscopy.

We first checked the sensitivity of the ^{19}F chemical shift of the tfmF23 group to changes in environment (Figure S1 of the Supporting Information) by examining the ^{19}F spectra in different environments. A detectable change was noticed for almost all changes in environment, including a substantial change in the chemical shift in urea, even though IAPP is considered to be natively unfolded.[52] The consumption of monomeric IAPP-tfmF$_{23}$ [initial concentration of 85 μM in 20 mM sodium phosphate and 50 mM NaCl (pH 7.3)] during amyloid fibrillogenesis was monitored by ^{19}F NMR (Figure 1). The monomeric peptide exhibits a single sharp peak near 14.7 ppm in the NMR spectrum. As expected, the signal intensity due to the monomeric peptide decreased in intensity over time in the characteristic sigmoidal manner observed in many studies of amyloid fiber formation.[55−57] No signal was observed from the large amyloid fibers as the peaks are broadened beyond detection. To determine the sensitivity of this method, the rate of monomer consumption was detected by measuring ^{19}F NMR signal intensity changes at three different temperatures: 10, 25, and 37 °C (Figure 1). As expected, both the lag time and elongation rate of fibril formation were temperature-dependent.[14,15,58] Even at higher temperatures (37 °C) and accelerated aggregation rates, we were able to monitor monomer consumption during aggregation efficiently using this technique.

IAPP-tfmF23 Forms Fibers from Monomers without the Accumulation of Nonfibrillar Intermediates. No additional peaks were observed in the ^{19}F spectrum of the peptide during the time course of the experiment, even at 10 °C where fibril formation is slowest (Figure 1). The position of the main resonance also did not change over the course of the experiment (Figure 1c), consistent with fluorescence studies that show Phe23 remains exposed during the lag phase of aggregation.[19] We also confirmed that tfmF23 is actually sensitive to the formation of small oligomers, were they to be formed in significant concentrations by cross-linking IAPP-tfmF$_{23}$ with EDC/sulfo-NHS.[59] In contrast to IAPP-tfmF$_{23}$ alone, additional peaks can clearly be seen downfield of the main peak when IAPP-tfmF$_{23}$ is incubated with 40 mM EDC/sulfo-NHS (Figure S2 of the Supporting Information). The intensity of the additional peaks increases with time as the magnitude of the main peak decreases (Figure S3 of the Supporting Information), confirming its presence is the result of the cross-linking reaction.

It is also important to note that even if an oligomer population cannot be directly detected by ^{19}F NMR because it is structurally inhomogeneous (which would broaden the signal), is too large to be detected by NMR, or the IAPP-tfmF23 ^{19}F NMR shift is unaffected by oligomerization, it still may be indirectly detected by a comparison of the monomer loss curves observed by ^{19}F NMR and the ThT and CD measurements of amyloid formation. If large oligomers or undetectable oligomers accumulate to a significant extent, a delay between the disappearance of the monomer (as measured by NMR) and the appearance of fibrils (as measured by ThT fluorescence and CD) would be observed.[21,60]

dx.doi.org/10.1021/bi3012548 | *Biochemistry* 2012, 51, 8154−8162

To test this possibility, we followed the aggregation of similarly prepared samples of IAPP-tfmF$_{23}$ by ThT fluorescence, CD spectroscopy, and ^{19}F NMR (Figure 2,

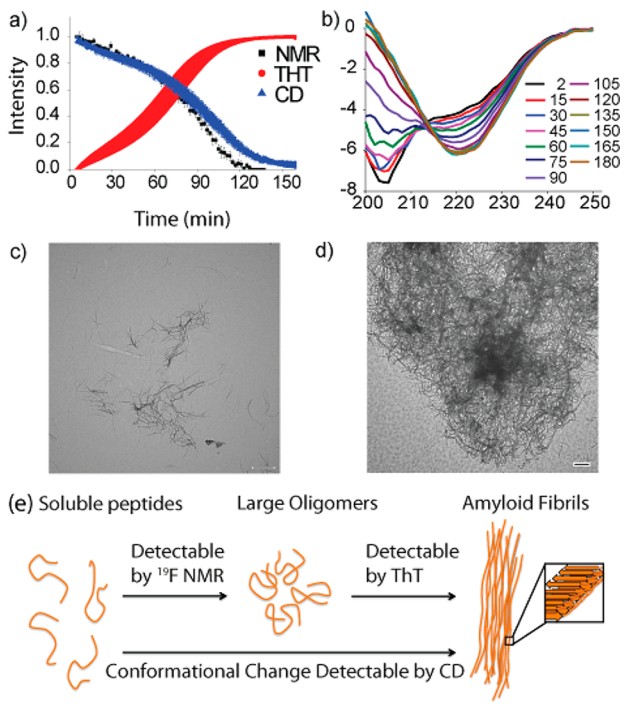

Figure 2. Comparison of the rates of monomer consumption and fiber formation. (a) Overlay of kinetic traces obtained via ^{19}F NMR (black), ThT fluorescence (red), and CD (blue). Solid lines represent sigmoidal fits to the ^{19}F and CD data. Error bars indicate the standard error of measurement (n = 4 for NMR and CD, and n = 5 for ThT). The close correspondence between the curves suggests fiber formation closely follows monomer consumption. (b) CD spectra showing the time evolution of secondary structure. (c and d) TEM images of IAPP-tfmF$_{23}$ after half-depletion (c) and complete depletion (d) of the ^{19}F signal intensity at 25 °C. Scale bars represent 500 nm. (e) Cartoon showing the sensitivities of each method.

parameters from the sigmoidal fit can be found in Table S1 of the Supporting Information). The rate of monomer consumption of IAPP-tfmF23 closely matches the rate of amyloid formation when experiments are performed at identical buffer and peptide concentrations at 25 and 37 °C (Figure 2 and Figure S4 of the Supporting Information). The ThT and NMR curves match well at 37 °C ($t_{1/2}$ = 18.8 ± 0.8 and 16.8 ± 1.6, respectively; p = 0.30), and the CD and NMR curves match very closely at 25 °C ($t_{1/2}$ = 91.8 ± 6.3 and 91.9 ± 3.1, respectively; p = 0.99). A relatively small in this context but statistically significant (p = 0.02) difference was observed between the ThT and NMR curves at 25 °C ($t_{1/2}$ = 64.3 ± 6.9 and 91.9 ± 3.1, respectively). This small difference in the kinetics between the two measurements may be caused by differences between the shape and size of the NMR tube and fluorescence cuvette, as interactions between the sample and container surfaces are known to nucleate amyloid formation.[61−63] This difference is magnified at the slower nucleation rates occurring at lower temperatures.[61]

The fact that the NMR, CD, and ThT curves closely track each other suggests the monomeric peptide is converted into a large, mostly β-sheet, ThT-reactive species without the accumulation of nonfibrillar intermediates. The absence of a substantial population of nonfibrillar oligomeric species along the aggregation pathway is notably different from what has been observed for many other amyloidogenic proteins.[16,64,65] For example, many intermediate species are formed during the aggregation of Aβ, including a distinct α-helical intermediate.[11,16,64−66] Systems that are known to have nonfibrillar oligomeric intermediates typically show a much larger difference in rates of monomer depletion and fiber formation. For example, the midpoints of the monomer consumption and fiber formation curves of Aβ can differ by 1 order of magnitude.[16] Similarly, monomer consumption and fiber formation curves of CsgA differ by a factor of 2.[21] The correspondence between the curves suggests any transient oligomers that are formed by IAPP-tfmF23 comprise only a minor population of the total at any given point in time.

The close coincidence of the midpoints of aggregation determined by the ^{19}F NMR and the ThT and CD measurements impose fairly stringent requirements on the type of nonfibrillar oligomers that can be formed. However, the data do not distinguish between certain kinetic mechanisms. For example, our data cannot exclude the presence of large, off-pathway oligomers whose concentration does not change appreciably in the lag phase of aggregation.[14,15] In addition, very transient oligomers that do not accumulate to a significant extent will not be observed in the experiment.[15]

TEM images acquired at the midpoints and end points of aggregation also support this conclusion (Figure 2c,d and Figure S5 of the Supporting Information). Images taken at the midpoint of aggregation show fibers that are similar in morphology to those found in at the end point but with a smaller density of fibers on the grid (Figure 2c and Figure S5a of the Supporting Information). Nonfibrillar aggregates large enough to be resolved in the TEM image, such as the spherical and annular intermediates frequently detected for α-synuclein and Aβ and implicated in toxicity, are noticeably absent.[6,66]

^{19}F NMR Measurement of the Interaction of Polyphenolic Inhibitors with IAPP without Interference from External Probes. Having demonstrated the utility of ^{19}F NMR to follow the kinetics of amyloid formation, we used it to investigate the mechanism by which EGCG (Figure 3a) inhibits IAPP-tfmF$_{23}$ amyloid formation. EGCG is the most abundant catechin found in tea and is a potent antioxidant, making it a potential therapeutic for many disorders. It has been reported that EGCG inhibits fiber formation in vitro for many amyloidogenic proteins, including Aβ, α-synuclein, and polyglutamine peptides.[67−72] Meng et al. recently showed that EGCG not only inhibits IAPP amyloid formation effectively but also is one of the few small molecule compounds that also disaggregates IAPP amyloid fibrils in vitro.[69] However, the mechanism of inhibition by EGCG is not known for IAPP.[69] Optical measurements of fiber inhibition by EGCG and other polyphenols are complicated by the background signal from these compounds and, potentially, by competitive binding with extrinsic probes like ThT.[68,73−76] In contrast, measurements of the rate of monomer consumption by ^{19}F NMR are easily quantified and are not affected by the nature of the inhibitor.

The kinetics of IAPP-tfmF23 aggregation were studied in the presence of 0.2, 0.5, 1.0, and 5.0 molar equiv of EGCG by ^{19}F NMR and ThT fluorescence (Figure 3b,c). It is apparent from both the ^{19}F and ThT measurements that EGCG inhibits fiber formation in a dose-dependent manner. However, a comparison of the data in panels b and c of Figure 3 reveals some

dx.doi.org/10.1021/bi3012548 | Biochemistry 2012, 51, 8154−8162

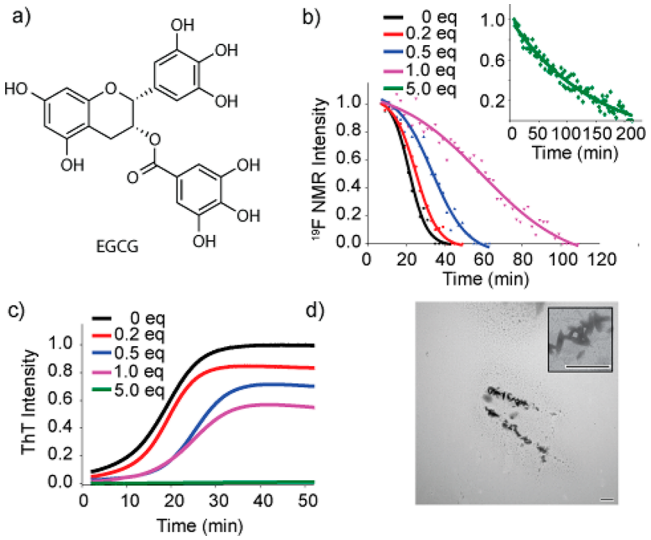

Figure 3. EGCG inhibits IAPP-tfmF_{23} amyloid fibrillogenesis. (a) Structure of EGCG. (b and c) Time courses for peptide aggregation followed by ^{19}F NMR (b) and ThT fluorescence (c) of IAPP-tfmF_{23} alone (85 μM, black) and at 1:5 (red) 1:2 (blue), 1:1 (magenta), and 5:1 (green) EGCG:IAPP molar ratios at pH 7.3 and 37 °C. Solid lines represent sigmoidal fits to the ^{19}F data; 100 μM ThT is present in the ThT samples (c) but is absent from the NMR samples (b). (d) TEM images of a 1:5 IAPP/EGCG mixture after the complete depletion of the ^{19}F signal intensity. The scale bar represents 500 nm.

important differences between the ThT and ^{19}F NMR measurements of the apparent effects of EGCG. When IAPP is incubated with an excess of EGCG (green lines in panels b and c of Figure 3), the ThT assay shows a complete inhibition of fiber formation while the ^{19}F NMR measurement shows a slow but steady decrease at longer time periods. This delay between the disappearance of the monomer and the appearance of fibrils is consistent with the production of large nonfibrillar aggregates that are not fluorescent when incubated with ThT.[67]

This interpretation is supported by the analysis of TEM images taken at the end points of aggregation, which show the appearance of large nonfibrillar aggregates at higher concentrations of EGCG but with a greatly reduced density of fibers (Figure 3d and Figure S6 of the Supporting Information). However, the TEM images are not definitive by themselves as EGCG by itself polymerizes over time to form aggregates with a morphology similar to that of the aggregates seen in Figure S6 (Figure S7 of the Supporting Information).[16] While the delay between the disappearance of the monomer and the appearance of fibrils is indicative of the formation of large nonfibrillar aggregates, substoichiometric amounts of EGCG shift the ^{19}F NMR curve to later times relative to ThT measurements (blue and pink curves in panels b and c of Figure 3, 0.5 and 1 equiv of EGCG, respectively). This result seems to imply that the monomer disappears after the appearance of fibrils at low EGCG concentrations. We believe that this apparent contradiction is due to interfence by EGCG with the ThT binding assay as discussed below.

Thioflavin T and EGCG Competitively Bind to IAPP Fibers. In Figure 3, 100 μM ThT is present during the ThT assay but not during the NMR measurements. To determine more accurately the effect of ThT on EGCG inhibition, we first determined if ThT by itself has any effect on amyloid aggregation. The rate of disappearance of the monomer was not significantly changed by the presence of ThT (Figure 4a), indicating that ThT by itself does not affect the kinetics of fiber formation.

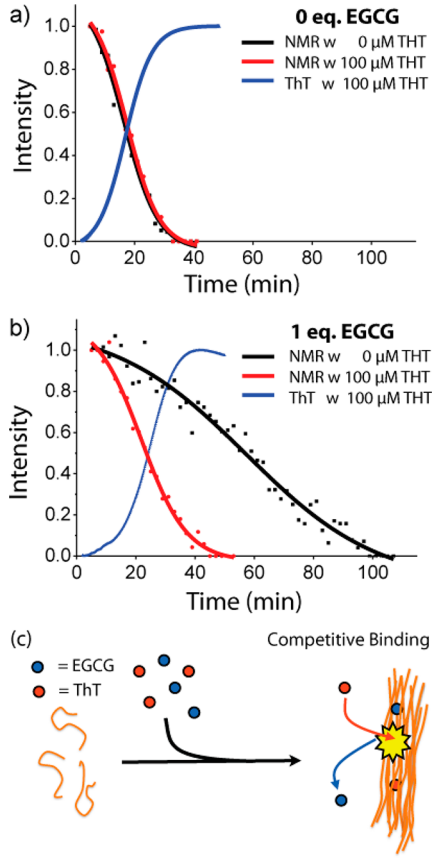

Figure 4. Competition for amyloid binding between ThT and EGCG. (a) Overlay of kinetic traces from ^{19}F NMR (black for 0 μM ThT and red for 100 μM ThT) and ThT fluorescence (blue for 100 μM ThT) without EGCG. Solid lines represent sigmoidal fits to the ^{19}F data. (b) Kinetic traces obtained under the same conditions but performed in the presence of 1 equiv of EGCG to peptide. Kinetic traces in the presence of 0.5 equiv of EGCG can be found in Figure S8 of the Supporting Information. (c) Cartoon schematic of the competitive binding effect.

However, although ThT has little effect on the rate of monomer depletion on its own, it may indirectly influence the rate of aggregation by significantly attenuating the inhibitory effect of EGCG. If ThT competes for the same binding site as EGCG on the amyloid fiber, the decrease in the amount of bound EGCG in the ThT assay would be reflected in lower levels of inhibition. This effect would not be observable when EGCG is in great excess of ThT (green lines panels b and c of Figure 3).

To check for this possibility, we performed the ^{19}F measurements using the same concentration of ThT as in the ThT assay [100 μM (Figure 4b and Figure S8 of the Supporting Information)]. In samples with EGCG, the addition of ThT causes a substantial shift of the NMR curves to earlier times, indicating monomer depletion happens at a faster rate in samples with EGCG when ThT is present (Figure 4b and Figure S8 of the Supporting Information). This shift is not observed in samples without EGCG (Figure 4a). This finding indicates that while ThT has little effect on the rate of aggregation by itself, it significantly attenuates the inhibitory

dx.doi.org/10.1021/bi3012548 | *Biochemistry* 2012, 51, 8154−8162

effect of EGCG, consistent with ThT effectively competing with EGCG for binding to IAPP fibrils. Similarly, the observation that high concentrations of EGCG prevent amyloid fiber formation (Figure 3c) may be attributed to the effective competition of EGCG for ThT binding sites when it is in sufficient excess over ThT.

EGCG Diverts Amyloid Aggregation to Nonfibrillar Aggregates. Given the many proposed modes of action of polyphenolic compounds against amyloidogenic proteins, it is difficult to determine the precise mechanism by which EGCG inhibits IAPP amyloid formation. The chemical shift of IAPP-tfmF23 was unchanged by the presence of either EGCG or ThT, indicating neither compound binds to the monomeric peptide, as has been proposed to happen for some amyloidogenic proteins (Figure S9 of the Supporting Information).[68,72,77,78]

As shown in Figure 4, competition between EGCG and ThT introduces significant artifacts when the ThT concentration is close to the peptide concentration. This is an important observation, because ThT is commonly used at relatively high concentrations in aggregation studies. However, when the concentration of ThT was lowered to 10 μM, competition between ThT and EGCG was weakened and it was possible to obtain accurate results for both the rate of fiber formation and monomer consumption (Figure 5). From the ^{19}F NMR results,

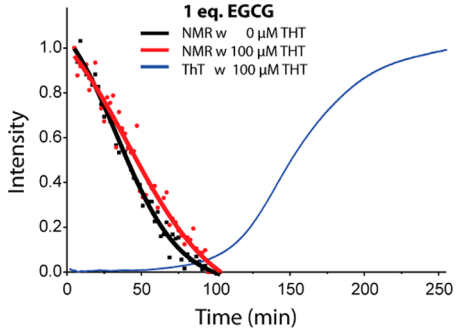

Figure 5. Competition between ThT and EGCG is weakened at lower ThT concentrations. Overlay of kinetic traces from ^{19}F NMR (black for 0 μM ThT and red for 10 μM ThT) and ThT fluorescence (blue for 10 μM ThT) with 1equiv of EGCG. Solid lines represent sigmoidal fits to the ^{19}F data.

it is apparent that the monomer is almost completely consumed in the presence of EGCG during the lag time before the formation of fibers (Figure 5). This result is striking contrast to the kinetics observed in the absence of EGCG, where fiber formation and monomer consumption occur simultaneously.

The delay between monomer consumption and fiber formation suggests that EGCG stabilizes the formation of nonfibrillar aggregates that are too large to be detected by NMR.[67] To test this possibility, we examined the reverse reaction by testing the ability of EGCG to disaggregate IAPP-tfmF23 amyloid fibrils using ^{19}F NMR and ThT fluorescence. As Figure 6a shows, the addition of a 5-fold molar excess of EGCG after the formation of IAPP amyloid fibrils caused a significant decrease in ThT fluorescence suggestive of the breakup of fibrils. However, no signals due to IAPP-tfmF$_{23}$ were observed by ^{19}F NMR after the addition of EGCG (Figure 6c), as would be expected if the fibers were completely broken up by EGCG to the monomeric peptide or small oligomers. An examination of the TEM images of supports this conclusion

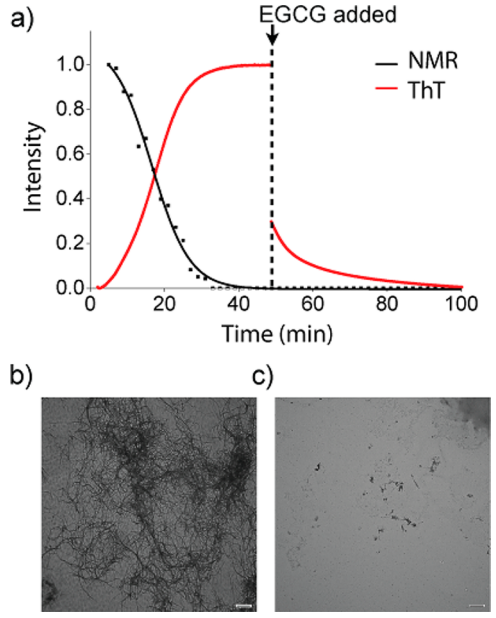

Figure 6. Disaggregation of amyloid fibrils due to the addition of EGCG. (a) Kinetic traces from ^{19}F NMR (black) and ThT fluorescence (red) measurements at 37 °C. Disaggregation of amyloid fibril formation was complete by the addition of 5 equiv of EGCG at the indicated time point. Solid lines represent sigmoidal fits to the ^{19}F data. (b) TEM image just before the addition of EGCG. (c) TEM image after the complete depletion of ThT fluorescence intensity (100 min). Scale bars represent 500 nm.

(Figure 6b and Figure S10 of the Supporting Information). TEM images taken at the end point of aggregation show small aggregates that are much shorter in length (Figure 6b and Figure S6 of the Supporting Information) than the regular fibers formed by IAPP (Figure 2 and Figure S5 of the Supporting Information) that are similar to those found with Aβ and α-synuclein incubated with EGCG. Instead of stabilizing the monomeric state, EGCG apparently diverts aggregation of IAPP toward large oligomers with a morphology different from that of the amyloid fiber. In this respect, the interaction of EGCG with IAPP is similar to many but not all of those of amyloidogenic proteins.[67,79,80]

■ CONCLUSIONS

These studies demonstrate the utility of using ^{19}F NMR to follow fibrillogenesis in real time by observing the rate of monomer consumption. Most of the methods typically used for monitoring the kinetics of aggregation measure the rate of appearance of the final product. By providing an additional independent measurement of the starting material, ^{19}F NMR can help distinguish between alternative pathways of aggregation, a task that is difficult to accomplish by other methods. Because fluorine is not found in most biological systems, there is no competition from background signals, a problem that often afflicts measurements using ^{1}H, ^{13}C, and ^{15}N NMR. The absence of a fluorophore simplifies detection and analysis of amyloid formation by other techniques. Therefore, the use of ^{19}F NMR should be applicable for automated screening of amyloid inhibitors without the false negative and positive results that might be present with other techniques.

dx.doi.org/10.1021/bi3012548 | Biochemistry 2012, 51, 8154−8162

■ ASSOCIATED CONTENT

Supporting Information

Complete ref 78, additional figures illustrating the kinetics of amyloid formation, ^{19}F spectra showing the environmental sensitivity of the tfmF23 group, ^{19}F spectra showing the formation of oligomers incubated with a cross-linking reagent, electron micrographs showing the morphologies of the IAPP aggregates in the presence and absence of EGCG, and a table of parameters derived from the sigmoidal fits. This material is available free of charge via the Internet at http://pubs.acs.org.

■ AUTHOR INFORMATION

Corresponding Author

*A.R.: Department of Chemistry, University of Michigan, Ann Arbor, MI 48109-1055; telephone, (734) 647-6572; fax, (734) 615-3790; e-mail, ramamoor@umich.edu. E.N.G.M.: Department of Chemistry, University of Michigan, Ann Arbor, MI 48109-1055; telephone, (734) 763-6096; fax, (734) 615-3790; e-mail, nmarsh@umich.edu.

Funding

This work was supported by grants from the National Institutes of Health (GM GM084018 and GM095640 to A.R.) and the Department of Defense Multidisciplinary University Research Initiative (DoD 59743-CH-MUR to E.N.G.M.).

Notes

The authors declare no competing financial interest.

■ ABBREVIATIONS

Aβ, amyloid-β; IAPP, islet amyloid polypeptide; ThT, thioflavin T; CD, circular dichroism; EGCG, (−)-epigallocatechin gallate; tfmF, trifluoromethylphenylalanine; Fmoc, fluorenylmethyloxycarbonyl; EDC, 1-ethyl-3-[3-(dimethylamino)propyl]-carbodiimide; sulfo-NHS, *N*-hydroxysulfosuccinimide; TFE, trifluoroethanol; TEM, transmission electron microscopy.

■ REFERENCES

(1) Chiti, F., and Dobson, C. M. (2006) Protein misfolding, functional amyloid, and human disease. *Annu. Rev. Biochem. 75*, 333−366.

(2) Luca, S., Yau, W. M., Leapman, R., and Tycko, R. (2007) Peptide conformation and supramolecular organization in amylin fibrils: Constraints from solid-state NMR. *Biochemistry 46*, 13505−13522.

(3) Nelson, R., and Eisenberg, D. (2006) Recent atomic models of amyloid fibril structure. *Curr. Opin. Struct. Biol. 16*, 260−265.

(4) Tycko, R. (2011) Solid-state NMR studies of amyloid fibril structure. *Annu. Rev. Phys. Chem. 62*, 279−299.

(5) Harrison, R. S., Sharpe, P. C., Singh, Y., and Fairlie, D. P. (2007) Amyloid peptides and proteins in review. *Rev. Physiol. Biochem. Pharmacol. 159*, 1−77.

(6) Ferreira, S. T., Vieira, M. N. N., and De Felice, F. G. (2007) Soluble protein oligomers as emerging toxins in Alzheimer's and other amyloid diseases. *IUBMB Life 59*, 332−345.

(7) Zraika, S., Hull, R. L., Verchere, C. B., Clark, A., Potter, K. J., Fraser, P. E., Raleigh, D. P., and Kahn, S. E. (2010) Toxic oligomers and islet beta cell death: Guilty by association or convicted by circumstantial evidence? *Diabetologia 53*, 1046−1056.

(8) Haataja, L., Gurlo, T., Huang, C. J., and Butler, P. C. (2008) Islet amyloid in type 2 diabetes, and the toxic oligomer hypothesis. *Endocr. Rev. 29*, 302−316.

(9) Lansbury, P. T., and Lashuel, H. A. (2006) A century-old debate on protein aggregation and neurodegeneration enters the clinic. *Nature 443*, 774−779.

(10) Capone, R., Quiroz, F. G., Prangkio, P., Saluja, I., Sauer, A. M., Bautista, M. R., Turner, R. S., Yang, J., and Mayer, M. (2009) Amyloid-β-induced ion flux in artificial lipid bilayers and neuronal cells: Resolving a controversy. *Neurotoxic. Res. 16*, 1−13.

(11) Chimon, S., Shaibat, M. A., Jones, C. R., Calero, D. C., Aizezi, B., and Ishii, Y. (2007) Evidence of fibril-like β-sheet structures in a neurotoxic amyloid intermediate of Alzheimer's β-amyloid. *Nat. Struct. Mol. Biol. 14*, 1157−1164.

(12) Yoshiike, Y., Minai, R., Matsuo, Y., Chen, Y. R., Kimura, T., and Takashima, A. (2008) Amyloid oligomer conformation in a group of natively folded proteins. *PLoS One 3*, e3235.

(13) Masuda, M., Hasegawa, M., Nonaka, T., Oikawa, T., Yonetani, M., Yamaguchi, Y., Kato, K., Hisanaga, S., and Goedert, M. (2009) Inhibition of α-synuclein fibril assembly by small molecules: Analysis using epitope-specific antibodies. *FEBS Lett. 583*, 787−791.

(14) Soong, R., Brender, J. R., Macdonald, P. M., and Ramamoorthy, A. (2009) Association of highly compact type II diabetes related islet amyloid polypeptide intermediate species at physiological temperature revealed by diffusion NMR spectroscopy. *J. Am. Chem. Soc. 131*, 7079−7085.

(15) Vaiana, S. M., Ghirlando, R., Yau, W. M., Eaton, W. A., and Hofrichter, J. (2008) Sedimentation studies on human amylin fail to detect low-molecular-weight oligomers. *Biophys. J. 94*, L45−L47.

(16) Lee, J., Culyba, E. K., Powers, E. T., and Kelly, J. W. (2011) Amyloid-β forms fibrils by nucleated conformational conversion of oligomers. *Nat. Chem. Biol. 7*, 602−609.

(17) Groenning, M. (2009) Binding mode of thioflavin T and other molecular probes in the context of amyloid fibrils: Current status. *J. Chem. Biol. 3*, 1−18.

(18) Marek, P., Gupta, R., and Raleigh, D. P. (2008) The fluorescent amino acid p-cyanophenylalanine provides an intrinsic probe of amyloid formation. *ChemBioChem 9*, 1372−1374.

(19) Marek, P., Mukherjee, S., Zanni, M. T., and Raleigh, D. P. (2010) Residue-specific, real-time characterization of lag-phase species and fibril growth during amyloid formation: A combined fluorescence and IR study of p-cyanophenylalanine analogs of islet amyloid polypeptide. *J. Mol. Biol. 400*, 878−888.

(20) Mishra, R., Geyer, M., and Winter, R. (2009) NMR spectroscopic investigation of early events in IAPP amyloid fibril formation. *ChemBioChem 10*, 1769−1772.

(21) Horvath, I., Weise, C. F., Andersson, E. K., Chorell, E., Sellstedt, M., Bengtsson, C., Olofsson, A., Hultgren, S. J., Chapman, M., Wolf-Watz, M., Almqvist, F., and Wittung-Stafshede, P. (2012) Mechanisms of protein oligomerization: Inhibitor of functional amyloids templates α-synuclein fibrillation. *J. Am. Chem. Soc. 134*, 3439−3444.

(22) Shim, S. H., Gupta, R., Ling, Y. L., Strasfeld, D. B., Raleigh, D. P., and Zanni, M. T. (2009) Two-dimensional IR spectroscopy and isotope labeling defines the pathway of amyloid formation with residue-specific resolution. *Proc. Natl. Acad. Sci. U.S.A. 106*, 6614−6619.

(23) Wang, L., Middleton, C. T., Singh, S., Reddy, A. S., Woys, A. M., Strasfeld, D. B., Marek, P., Raleigh, D. P., de Pablo, J. J., Zanni, M. T., and Skinner, J. L. (2011) 2DIR spectroscopy of human amylin fibrils reflects stable β-sheet structure. *J. Am. Chem. Soc. 133*, 16062−16071.

(24) Larson, J. L., Ko, E., and Miranker, A. D. (2000) Direct measurement of islet amyloid polypeptide fibrillogenesis by mass spectrometry. *Protein Sci. 9*, 427−431.

(25) Cole, H. L., Kalapothakis, J. M. D., Bennett, G., Barran, P. E., and MacPhee, C. E. (2010) Characterizing early aggregates formed by an amyloidogenic peptide by mass spectrometry. *Angew. Chem., Int. Ed. 49*, 9448−9451.

(26) Maezawa, I., Hong, H. S., Liu, R., Wu, C. Y., Cheng, R. H., Kung, M. P., Kung, H. F., Lam, K. S., Oddo, S., LaFerla, F. M., and Jin, L. W. (2008) Congo red and thioflavin-T analogs detect Aβ oligomers. *J. Neurochem. 104*, 457−468.

(27) Cobb, S. L., and Murphy, C. D. (2009) ^{19}F NMR applications in chemical biology. *J. Fluorine Chem. 130*, 132−143.

(28) Salwiczek, M., Nyakatura, E. K., Gerling, U. I. M., Ye, S., and Koksch, B. (2012) Fluorinated amino acids: Compatibility with native protein structures and effects on protein-protein interactions. *Chem. Soc. Rev. 41*, 2135−2171.

(29) Bann, J. G., Pinkner, J., Hultgren, S. J., and Frieden, C. (2002) Real-time and equilibrium F-19-NMR studies reveal the role of domain-domain interactions in the folding of the chaperone papd. *Proc. Natl. Acad. Sci. U.S.A. 99*, 709−714.
(30) Li, H. L., and Frieden, C. (2007) Observation of sequential steps in the folding of intestinal fatty acid binding protein using a slow folding mutant and F-19 NMR. *Proc. Natl. Acad. Sci. U.S.A. 104*, 11993−11998.
(31) Li, H., and Frieden, C. (2007) Comparison of C40/82A and P27A C40/82A barstar mutants using F-19 NMR. *Biochemistry 46*, 4337−4347.
(32) Schlesinger, A. P., Wang, Y. Q., Tadeo, X., Millet, O., and Pielak, G. (2011) Macromolecular crowding fails to fold a globular protein in cells. *J. Am. Chem. Soc. 133*, 8082−8085.
(33) Anderluh, G., Razpotnik, A., Podlesek, Z., Macek, P., Separovic, F., and Norton, R. S. (2005) Interaction of the eukaryotic pore-forming cytolysin equinatoxin II with model membranes: F-19 NMR studies. *J. Mol. Biol. 347*, 27−39.
(34) Glaser, R. W., Sachse, C., Durr, U. H. N., Wadhwani, P., and Ulrich, A. S. (2004) Orientation of the antimicrobial peptide PGLa in lipid membranes determined from F-19-NMR dipolar couplings of 4-CF3-phenylglycine labels. *J. Magn. Reson. 168*, 153−163.
(35) Afonin, S., Grage, S. L., Ieronimo, M., Wadhwani, P., and Ulrich, A. S. (2008) Temperature-dependent transmembrane insertion of the amphiphilic peptide PGLa in lipid bilayers; observed by solid state ^{19}F NMR spectroscopy. *J. Am. Chem. Soc. 130*, 16512−16514.
(36) Suzuki, Y., Buer, B. C., Al-Hashimi, H. M., and Marsh, E. N. G. (2011) Using fluorine nuclear magnetic resonance to probe changes in the structure and dynamics of membrane-active peptides interacting with lipid bilayers. *Biochemistry 50*, 5979−5987.
(37) Buer, B. C., Chugh, J., Al-Hashimi, H. M., and Marsh, E. N. G. (2010) Using fluorine nuclear magnetic resonance to probe the interaction of membrane-active peptides with the lipid bilayer. *Biochemistry 49*, 5760−5765.
(38) Li, C. G., Wang, G. F., Wang, Y. Q., Creager-Allen, R., Lutz, E. A., Scronce, H., Slade, K. M., Ruf, R. A. S., Mehl, R. A., and Pielak, G. J. (2010) Protein ^{19}F NMR in *Escherichia coli*. *J. Am. Chem. Soc. 132*, 321−327.
(39) Jackson, J. C., Hammill, J. T., and Mehl, R. A. (2007) Site-specific incorporation of a ^{19}F-amino acid into proteins as an NMR probe for characterizing protein structure and reactivity. *J. Am. Chem. Soc. 129*, 1160−1166.
(40) Shi, P., Wang, H., Xi, Z. Y., Shi, C. W., Xiong, Y., and Tian, C. L. (2011) Site-specific ^{19}F NMR chemical shift and side chain relaxation analysis of a membrane protein labeled with an unnatural amino acid. *Protein Sci. 20*, 224−228.
(41) Liu, J. J., Horst, R., Katritch, V., Stevens, R. C., and Wuthrich, K. (2012) Biased signaling pathways in β2-adrenergic receptor characterized by ^{19}F-NMR. *Science 335*, 1106−1110.
(42) Jackel, C., Salwiczek, M., and Koksch, B. (2006) Fluorine in a native protein environment: How the spatial demand and polarity of fluoroalkyl groups affect protein folding. *Angew. Chem., Int. Ed. 45*, 4198−4203.
(43) Salwiczek, M., Mikhailiuk, P. K., Afonin, S., Komarov, I. V., Ulrich, A. S., and Koksch, B. (2010) Compatibility of the conformationally rigid CF3-Bpg side chain with the hydrophobic coiled-coil interface. *Amino Acids 39*, 1589−1593.
(44) Li, C. G., Lutz, E. A., Slade, K. M., Ruf, R. A. S., Wang, G. F., and Pielak, G. J. (2009) ^{19}F NMR studies of α-synuclein conformation and fibrillation. *Biochemistry 48*, 8578−8584.
(45) Maisch, D., Wadhwani, P., Afonin, S., Boettcher, C., Koksch, B., and Ulrich, A. S. (2009) Chemical labeling strategy with (R)- and (S)-trifluoromethylalanine for solid state ^{19}F NMR analysis of peptaibols in membranes. *J. Am. Chem. Soc. 131*, 15596.
(46) Westermark, P., Andersson, A., and Westermark, G. T. (2011) Islet amyloid polypeptide, islet amyloid, and diabetes mellitus. *Physiol. Rev. 91*, 795−826.
(47) Hoppener, J. W. M., Ahren, B., and Lips, C. J. M. (2000) Islet amyloid and type 2 diabetes mellitus. *N. Engl. J. Med. 343*, 411−419.
(48) Brender, J. R., Salamekh, S., and Ramamoorthy, A. (2012) Membrane disruption and early events in the aggregation of the diabetes related peptide IAPP from a molecular perspective. *Acc. Chem. Res. 45*, 454−462.
(49) Page, K., Hood, C. A., Patel, H., Fuentes, G., Menakuru, M., and Park, J. H. (2007) Fast Fmoc synthesis of hAmylin(1−37) with pseudoproline assisted on-resin disulfide formation. *J. Pept. Sci. 13*, 833−838.
(50) Pace, C. N., Vajdos, F., Fee, L., Grimsley, G., and Gray, T. (1995) How to measure and predict the molar absorption-coefficient of a protein. *Protein Sci. 4*, 2411−2423.
(51) Brender, J. R., Hartman, K., Nanga, R. P., Popovych, N., de la Salud Bea, R., Vivekanandan, S., Marsh, E. N., and Ramamoorthy, A. (2010) Role of zinc in human islet amyloid polypeptide aggregation. *J. Am. Chem. Soc. 132*, 8973−8983.
(52) Yonemoto, I. T., Kroon, G. J., Dyson, H. J., Balch, W. E., and Kelly, J. W. (2008) Amylin proprotein processing generates progressively more amyloidogenic peptides that initially sample the helical state. *Biochemistry 47*, 9900−9910.
(53) Wiltzius, J. J. W., Sievers, S. A., Sawaya, M. R., Cascio, D., Popov, D., Riekel, C., and Eisenberg, D. (2008) Atomic structure of the cross-β spine of islet amyloid polypeptide (amylin). *Protein Sci. 17*, 1467−1474.
(54) Wiltzius, J. J., Sievers, S. A., Sawaya, M. R., and Eisenberg, D. (2009) Atomic structures of IAPP (amylin) fusions suggest a mechanism for fibrillation and the role of insulin in the process. *Protein Sci. 18*, 1521−1530.
(55) Linse, B., and Linse, S. (2011) Monte Carlo simulations of protein amyloid formation reveal origin of sigmoidal aggregation kinetics. *Mol. BioSyst. 7*, 2296−2303.
(56) Kodaka, M. (2004) Requirements for generating sigmoidal time-course aggregation in nucleation-dependent polymerization model. *Biophys. Chem. 107*, 243−253.
(57) Jarrett, J. T., and Lansbury, P. T. (1993) Seeding one-dimensional crystallization of amyloid: A pathogenic mechanism in Alzheimer's disease and scrapie. *Cell 73*, 1055−1058.
(58) Kayed, R., Bernhagen, J., Greenfield, N., Sweimeh, K., Brunner, H., Voelter, W., and Kapurniotu, A. (1999) Conformational transitions of islet amyloid polypeptide (IAPP) in amyloid formation in vitro. *J. Mol. Biol. 287*, 781−796.
(59) Schulz, D. M., Ihling, C., Clore, G. M., and Sinz, A. (2004) Mapping the topology and determination of a low-resolution three-dimensional structure of the calmodulin-melittin complex by chemical cross-linking and high-resolution FTICRMS: Direct demonstration of multiple binding modes. *Biochemistry 43*, 4703−4715.
(60) Powers, E. T., and Powers, D. L. (2006) The kinetics of nucleated polymerizations at high concentrations: Amyloid fibril formation near and above the "supercritical concentration". *Biophys. J. 91*, 122−132.
(61) Giehm, L., and Otzen, D. E. (2010) Strategies to increase the reproducibility of protein fibrillization in plate reader assays. *Anal. Biochem. 400*, 270−281.
(62) Jean, L., Lee, C. F., Lee, C., Shaw, M., and Vaux, D. J. (2010) Competing discrete interfacial effects are critical for amyloidogenesis. *FASEB J. 24*, 309−317.
(63) Pronchik, J., He, X. L., Giurleo, J. T., and Talaga, D. S. (2010) In vitro formation of amyloid from α-synuclein is dominated by reactions at hydrophobic interfaces. *J. Am. Chem. Soc. 132*, 9797−9803.
(64) Kirkitadze, M. D., Condron, M. M., and Teplow, D. B. (2001) Identification and characterization of key kinetic intermediates in amyloid β-protein fibrillogenesis. *J. Mol. Biol. 312*, 1103−1119.
(65) Ding, H., Wong, P. T., Lee, E. L., Gafni, A., and Steel, D. G. (2009) Determination of the oligomer size of amyloidogenic protein β-amyloid(1−40) by single-molecule spectroscopy. *Biophys. J. 97*, 912−921.
(66) Lambert, M. P., Barlow, A. K., Chromy, B. A., Edwards, C., Freed, R., Liosatos, M., Morgan, T. E., Rozovsky, I., Trommer, B., Viola, K. L., Wals, P., Zhang, C., Finch, C. E., Krafft, G. A., and Klein, W. L. (1998) Diffusible, nonfibrillar ligands derived from Aβ(1−42)

are potent central nervous system neurotoxins. *Proc. Natl. Acad. Sci. U.S.A. 95*, 6448−6453.
(67) Ehrnhoefer, D. E., Bieschke, J., Boeddrich, A., Herbst, M., Masino, L., Lurz, R., Engemann, S., Pastore, A., and Wanker, E. E. (2008) EGCG redirects amyloidogenic polypeptides into unstructured, off-pathway oligomers. *Nat. Struct. Mol. Biol. 15*, 558−566.
(68) Popovych, N., Brender, J. R., Soong, R., Vivekanandan, S., Hartman, K., Basrur, V., Macdonald, P. M., and Ramamoorthy, A. (2012) Site specific interaction of the polyphenol EGCG with the SEVI amyloid precursor peptide PAP(248−286). *J. Phys. Chem. B 116*, 3650−3658.
(69) Meng, F. L., Abedini, A., Plesner, A., Verchere, C. B., and Raleigh, D. P. (2010) The flavanol (−)-epigallocatechin 3-gallate inhibits amyloid formation by islet amyloid polypeptide, disaggregates amyloid fibrils, and protects cultured cells against IAPP-induced toxicity. *Biochemistry 49*, 8127−8133.
(70) Ferreira, N., Cardoso, I., Domingues, M. R., Vitorino, R., Bastos, M., Bai, G. Y., Saraiva, M. J., and Almeida, M. R. (2009) Binding of epigallocatechin-3-gallate to transthyretin modulates its amyloidogenicity. *FEBS Lett. 583*, 3569−3576.
(71) Hauber, I., Hohenberg, H., Holstermann, B., Hunstein, W., and Hauber, J. (2009) The main green tea polyphenol epigallocatechin-3-gallate counteracts semen-mediated enhancement of HIV infection. *Proc. Natl. Acad. Sci. U.S.A. 106*, 9033−9038.
(72) Huang, R., Vivekanandan, S., Brender, J. R., Abe, Y., Naito, A., and Ramamoorthy, A. (2012) NMR characterization of monomeric and oligomeric conformations of human calcitonin and its interaction with EGCG. *J. Mol. Biol. 416*, 108−120.
(73) Hudson, S. A., Ecroyd, H., Kee, T. W., and Carver, J. A. (2009) The thioflavin T fluorescence assay for amyloid fibril detection can be biased by the presence of exogenous compounds. *FEBS J. 276*, 5960−5972.
(74) Chandrashekaran, I. R., Adda, C. G., MacRaild, C. A., Anders, R. F., and Norton, R. S. (2011) EGCG disaggregates amyloid-like fibrils formed by *Plasmodium falciparum* merozoite surface protein 2. *Arch. Biochem. Biophys. 513*, 153−157.
(75) Liu, K. N., Wang, H. Y., Chen, C. Y., and Wang, S. S. S. (2010) L-Arginine reduces thioflavin T fluorescence but not fibrillation of bovine serum albumin. *Amino Acids 39*, 821−829.
(76) Meng, F., Marek, P., Potter, K. J., Verchere, C. B., and Raleigh, D. P. (2008) Rifampicin does not prevent amyloid fibril formation by human islet amyloid polypeptide but does inhibit fibril thioflavin-T interactions: Implications for mechanistic studies of β-cell death. *Biochemistry 47*, 6016−6024.
(77) Hudson, S. A., Ecroyd, H., Dehle, F. C., Musgrave, I. F., and Carver, J. A. (2009) (−)-Epigallocatechin-3-gallate (EGCG) maintains κ-casein in its pre-fibrillar state without redirecting its aggregation pathway. *J. Mol. Biol. 392*, 689−700.
(78) Miyata, M., et al. (2010) The crystal structure of the green tea polyphenol (−)-epigallocatechin gallate-transthyretin complex reveals a novel binding site distinct from the thyroxine binding site. *Biochemistry 49*, 6104−6114.
(79) Bieschke, J., Russ, J., Friedrich, R. P., Ehrnhoefer, D. E., Wobst, H., Neugebauer, K., and Wankeraaa, E. E. (2010) EGCG remodels mature α-synuclein and amyloid-β fibrils and reduces cellular toxicity. *Proc. Natl. Acad. Sci. U.S.A. 107*, 7710−7715.
(80) He, J., Xing, Y. F., Huang, B., Zhang, Y. Z., and Zeng, C. M. (2009) Tea catechins induce the conversion of preformed lysozyme amyloid fibrils to amorphous aggregates. *J. Agric. Food Chem. 57*, 11391−11396.